



A 3D printed acoustofluidic nozzle-diffuser microfluidic pump

Erturan Yetiskin¹ · Sinan Gucluer¹ · Ilayda Erdem¹ · Adem Ozcelik¹

Received: 5 January 2024 / Accepted: 12 March 2024
© The Author(s) 2024

Abstract

Microfluidic flow control systems are critical components for on-chip biomedical applications. This study introduces a new micropump for on-chip sample preparation and analysis by using an acoustic nozzle diffuser mechanism. The micropump implements a commercially available transducer and control board kit with 3D-printed fluid reservoirs. In this micropump, conic-shaped micro-holes on the metal sheet cover of the transducer are employed as oscillating nozzle diffuser micro arrays to achieve directional flow control. The micropump is shown to efficiently pump water and particle mixtures exceeding flow rates of 515 $\mu\text{l}/\text{min}$ at a 12-volt input voltage. In addition, owing to the small size of the nozzle hole opening, larger particles can also be filtered out from a sample solution during fluid pumping enabling a new function. Importantly, the micropump can be fabricated and assembled without needing a cleanroom, making it more accessible. This feature is advantageous for researchers and practitioners, eliminating a significant barrier to entry. By combining commercially available components with 3D printing technology, this micropump presents a cost-effective and versatile solution for on-chip applications in biomedical research and analysis.

Keywords Microfluidic pump · Acoustofluidics · Nozzle diffuser · 3D printed microfluidics

1 Introduction

In the realm of microfluidics, the relentless pursuit of miniature and cost-effective pumping solutions has been a driving force behind advancements in various fields, from biomedical diagnostics to chemical analysis (Xu et al. 2020; Cook et al. 2022; Li et al. 2023b). The inherent challenges associated with developing efficient microfluidic pumps that balance performance, affordability, and simplicity have fueled the exploration of various actuation mechanisms (Hossan et al. 2018; Li et al. 2019). However, the microfluidic pumps developed thus far have certain limitations such that the intricate designs and complex fabrication processes involved make these pumps less than ideal for widespread adoption. Furthermore, the lack of standardized protocols and

the nuanced nature of their assembly present significant hurdles for other researchers attempting to reproduce these pumps in resource-limited environments (Akkoyun et al. 2021). There is a need for the development of an easy-to-reproduce microfluidic pump that is not only simple and efficient but also addresses the current limitations, facilitating broader accessibility and accelerating progress in microfluidics research.

Over the years, the significance and potential of miniaturized bioanalytical systems have become increasingly evident, particularly in the context of their crucial role in addressing urgent and time-sensitive scenarios such as disease outbreaks and rapid disease screening (Cai et al. 2021; Ao et al. 2022; Lu et al. 2022; Wu et al. 2023b). These systems, often integrated into lab-on-chip platforms, offer unprecedented advantages in terms of portability, efficiency, and rapidity of analysis (Lin et al. 2019a; Gao et al. 2020b; Cai et al. 2021; Ozcelik and Aslan 2022; Wu et al. 2023a, c). Their ability to perform complex biological assays and diagnostic tests within compact and automated frameworks makes them invaluable tools for on-the-spot

✉ Adem Ozcelik
aozcelik@adu.edu.tr

¹ Department of Mechanical Engineering, Aydin Adnan Menderes University, Aydin, Turkey

testing, significantly reducing the time required for obtaining critical results (Gandotra et al. 2023; Li et al. 2023a). However, the seamless functionality of these lab-on-chip systems heavily relies on the development of efficient and simple microfluidic pumps (Iverson and Garimella 2008). These pumps are essential for precisely manipulating fluid flow within the microscale environment, enabling accurate and controlled sample transport and analysis. As technological advancements continue, the integration of efficient microfluidic pumps becomes pivotal in harnessing the full potential of miniaturized bioanalytical systems for swift and reliable diagnostics in critical situations.

Researchers have strived to enhance the performance, efficiency, and versatility of microfluidic pumps, addressing issues such as flow control, reliability, and integration with complex microscale systems. In this endeavor, both passive and active fluid actuation mechanisms have been integrated into microfluidic pumps to achieve controllable fluid flow manipulation (Berthier and Beebe 2007; Resto et al. 2012; Gao et al. 2020a; Ozcelik and Aslan 2021; Zhao et al. 2021; Gucluer 2021). Passive microfluidic pumps, driven by capillary forces, surface tension, and other inherent properties of fluids, have emerged as promising tools for achieving continuous flow within microscale systems (Chao and Meldrum 2009; Jeong et al. 2014; Guo et al. 2018). These pumps are simpler in terms of actuation mechanisms and device fabrication compared to externally powered micropumps, but they are limited in terms of flow rate control. As opposed to the passive micropumps, various external fields have been implemented in active microfluidic pumps including magnetic, electric, optic, peristaltic, and acoustic pumps (Bart et al. 1990; Leach et al. 2006; Iverson and Garimella 2008; Wang et al. 2017; Li et al. 2019; Binsley et al. 2020; Akkoyun and Ozcelik 2022). For example, various techniques have been employed to employ magnetic fields for microfluidic pumping, encompassing cilia actuation, magnetohydrodynamics, ferrofluidic actuation, and membrane actuation (Zhang et al. 2007; Hanasoge et al. 2018; Chen et al. 2020). In general, magnetic field-based micropumps rely on a rotating magnetic field and micro-actuation mechanisms that result in a relatively complex device architecture. Electrokinetic-based micropumps such as dielectrophoresis, electroosmosis, induced charge electroosmosis, and electrophoresis enable miniaturized fluid manipulation mechanisms through various electrode

geometries (Vafaie et al. 2016; Hossan et al. 2018). While these micropumps have been shown to provide precise flow manipulation capabilities, their fabrication process is fairly complex, and they usually depend on medium conductivity.

Acoustically driven micropumps have also been widely explored for microfluidic flow manipulation applications (Wang et al. 2010; Tovar et al. 2011; Wu et al. 2019). The driving force of attention for these systems arises from their non-invasiveness and label-free characteristics (Neild 2016; Ao et al. 2021). Acoustofluidics relies on two fundamental forces which are the acoustic radiation force and the drag force induced by acoustic streaming. Acoustic radiation forces primarily result from gradients due to scattering, reflection, dampening, interference, or absorption of acoustic waves (Bruus 2012; Karlsen et al. 2016), while acoustic streaming emerges from the viscous attenuation of acoustic waves within a fluid medium (Friend and Yeo 2011). Various mechanisms, such as surface acoustic wave-based localized streaming (Wu et al. 2019), trapped microbubble-based microstreaming (Tovar et al. 2011; Gao et al. 2020a), and sharp edge-based acoustic streaming (Huang et al. 2014; Nama et al. 2014; Doinikov et al. 2020), have been explored to generate acoustic streaming and facilitate fluid pumping. Even though acoustofluidics micropumps are versatile in terms of their functionalities, they usually still require expensive clean-room fabrication facilities. Therefore, there is still a need for a simple, low-cost, and efficient micropump that can easily be replicated in any laboratory with only 3D-printed parts and off-the-shelf components.

This manuscript introduces a new approach to microfluidic pumping, presenting a low-cost acoustofluidic nozzle diffuser microfluidic pump that leverages the controlled vibrations of micro nozzles to induce unidirectional fluid flow. All the electronic and mechanical parts implemented in this pump can easily be acquired and casing can be 3d printed. The demonstrated pumping mechanism relies on fluid flow resistance through an oscillating nozzle and could generate flow rates exceeding 515 $\mu\text{l}/\text{min}$ at only 12 volts applied voltage. In addition to its pumping function, the demonstrated system also provides efficient filtration of the pumped fluid eliminating any particles larger than the diameter of the nozzle-end. Overall, the demonstrated system is low-cost, simple, and versatile which can be applied to sample processing and bioanalyses.

2 Experimental methods

2.1 Device fabrication and assembly

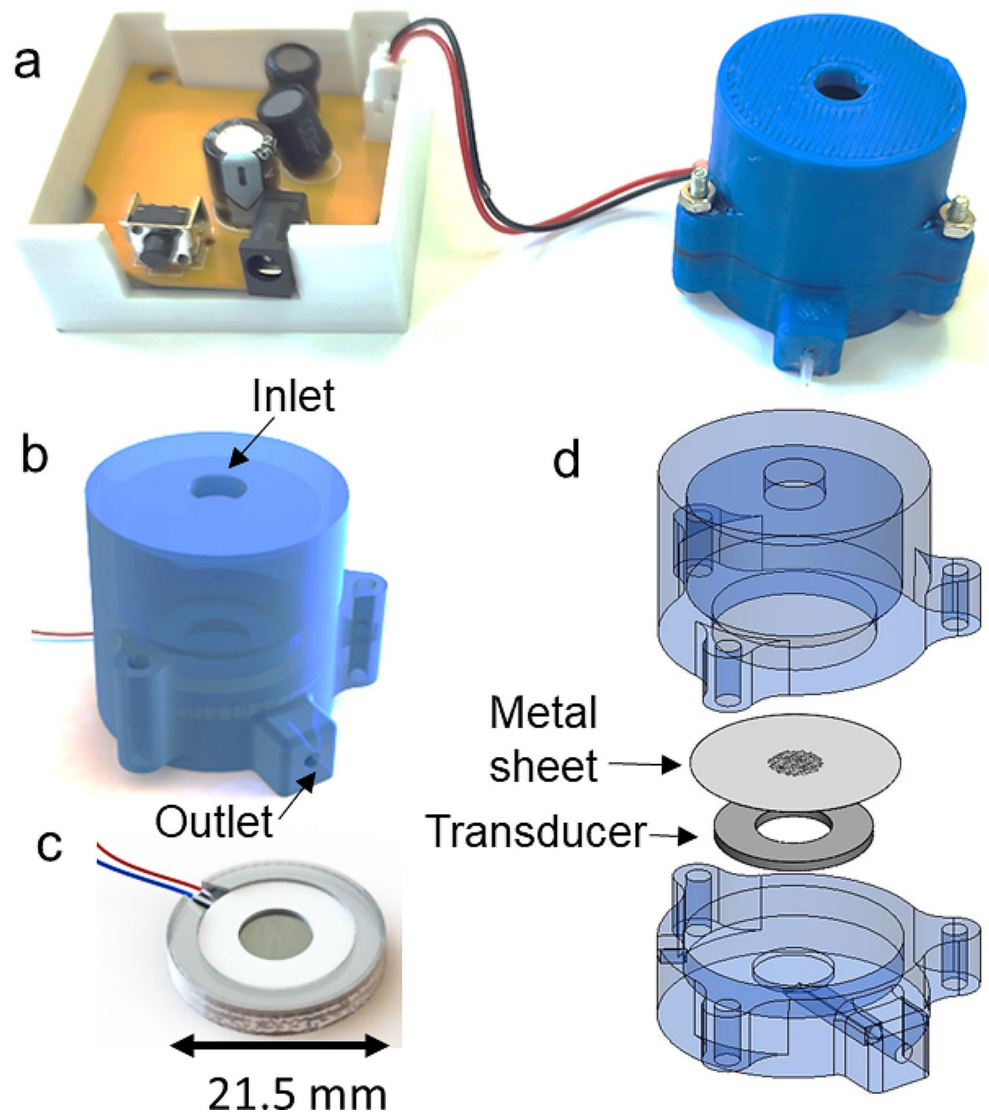
The presented device is designed to have three main parts including a top reservoir, an acoustic transducer, and a lower channel for fluid collection. The top reservoir and the bottom channel were designed to have three symmetric through holes for metric 3 screws that pressed the transducer in a silicone case for liquid-tight assembly. The reservoir and fluid collection parts were printed using a consumer-grade 3D printer (Ender 3 S1, Creality, Shenzhen, China). The parts were printed using 100% infill, 50 mm/s print speed, 0.8 mm retraction, -0.18 mm layer height, 210 °C nozzle temperature, and 60 °C print bed temperature. The STL files for these parts are provided as supplementary material for reproducing the micropump (Online Resource 1). The transducer and control board are off-the-shelf items commonly

used for ultrasonic mist generation (113 kHz, TaiMi, Guangdong, China). The transducer is ring-shaped and contains a 0.15 mm thick metal sheet with an array of conical holes. In the device assembly, the transducer was placed in a way that the larger holes (that are barely visible to the naked eye) on the metal cover sheet were facing toward the pumping channel. The controller board features an on-off switch and a 3 mm barrel jack for DC input. The controller can drive a 113 kHz transducer and can be powered by a simple DC power source such as a battery or power bank with voltages up to 12 Volts. The assembled device, the controller board, and device schematics are shown in Fig. 1.

2.2 Experimental setup

For pumping behavior visualization, a solution of filtered bottled water and a mixture containing 5 μm and larger (between 20 and 40 μm diameter) polystyrene microparticles

Fig. 1 Acoustic nozzle diffuser micropump picture and schematics. (a) Actual picture of the pumping device and electronic board. (b) Schematic depiction of the assembled device. (c) Schematic depiction of the acoustic transducer. (d) Exploded view of the device assembly showing top reservoir, metal sheet, transducer and bottom channel



(Sigma Aldrich, MO, United States) was used. For visual observation of fluid pumping, food dye and water were used. For characterization of the flow rates, the micropump outlet is connected to a 0.5 mm by 0.5 mm inner cross-section rectangular glass capillary (Vitrocom, NJ, USA) using silicone tubing. Motion of microparticles was captured using an inverted optical microscope (OX.2053-PLPH, Euromex, Arnhem, Netherlands) equipped with an HD camera (HD-Ultra, Euromex, Arnhem, Netherlands) and a portable camera (Note 10 Pro, Xiaomi, Beijing, China). The flow rates at different applied voltages were calculated by tracing the particles using ImageJ and calculating the velocities. Then, the channel cross-section is multiplied by the particle velocity to obtain volumetric flow rates. The surface of the thin metal sheet was imaged using an inverted metal microscope (XJP-6 A, Soif, Guangzhou, China) equipped with a CMOS camera (MS60, M-Shot, Guangzhou, China). A DC power supply (SPD-3606, GW-Instek, Taiwan) was used to characterize pumping performance as a function of applied DC voltage.

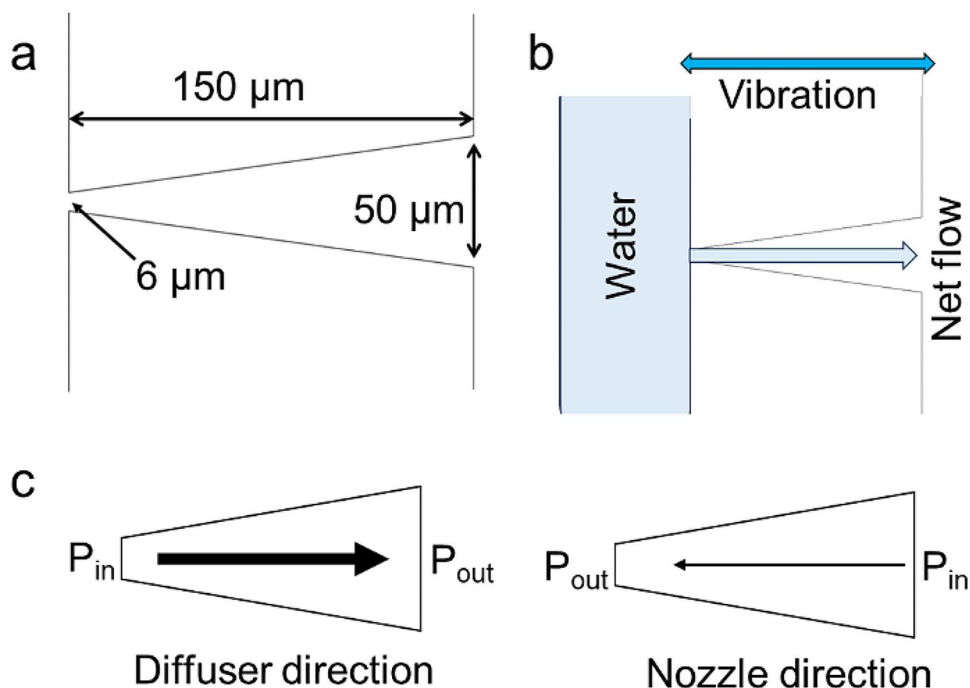
3 Results and discussions

3.1 Working mechanism

The proposed device is a valveless micropump based on a nozzle-diffuser mechanism (Fig. 2). For this, a thin metal sheet with approximately conic-shaped holes (as shown in

Figs. 2 and 3) that is attached to the center of a ringed-shaped transducer oscillates at about 113 kHz. When the water reservoir is placed at the nozzle side that has 6 μm diameter orifices, a net flow occurs towards the diffuser direction that has an array of holes with a diameter of 50 μm . This mechanism is frequently used in nozzle-diffuser-type microfluidic pumps, but they implement an elastic membrane and an intermediate chamber (Singhal et al. 2004; Ahmadian and Mehrabian 2006; Nisar et al. 2008; Li et al. 2013; Zhao et al. 2017). In traditional nozzle-diffuser pumps, the chamber is first supplied with fluid by diffuser action during a chamber volume expansion, and then the fluid is pumped through the second diffuser during the chamber volume contraction. In both volume expansion and contraction of the chamber, nozzle directions provide fluid resistance thus a net flow can be obtained in the diffuser direction. In our micropump, the micro diffuser array that is on the metal sheet rapidly travels back and forth towards and away from the fluid reservoir. This motion provides a stable directional pumping effect with controllable flow rates by tuning the amplitude of the oscillations. It is also important to note that vibrating boundaries can generate acoustic streaming within a fluid domain due to viscous damping. In our device, since the metal sheet oscillates in the fluid medium, acoustic streaming flows are expected to contribute to fluid manipulation. We observed movement of small dust particles due to the acoustic streaming within the pumped fluid in an experiment using an open system with only the transducer and metal sheet in contact with a fluid container (Online Resource 2)

Fig. 2 Schematic depiction of the dimensions and the working mechanism of the acoustic nozzle-diffuser micropump. (a) Cross-sectional view of a micro-hole with the actual diameters. (b) Water reservoir is placed on the nozzle side and a net flow occurs during membrane vibration. (c) Diffuser action provides less fluid resistance and a net flow while nozzle action restricts the flow by higher flow resistance



which is occurring mostly due to the oscillating boundaries of 50 μm holes on the metal sheet.

For this microfluidic pump, we took advantage of a commercially available and low-cost mist generation unit. For mist generation, the water reservoir is placed on the diffuser side that has the larger diameter holes, and water moves through the nozzle to a lower pressure side and turns into mist (Zhang et al. 2018; Guerra-Bravo et al. 2021). In our system, we designed a pumping channel for the diffuser direction (Fig. 3a and b) and a fluid reservoir for the nozzle direction (Fig. 3c and d). When no voltage is applied to the controller, the transducer does not oscillate, and no fluid flow occurs through the micro-hole array. By applying increasing values of voltages up to 12 volts, the transducer oscillates, and a controllable fluid flow is provided toward the diffuser direction.

3.2 Pumping characterization

The developed pumping system was shown to provide directional fluid pumping using both visual demonstration (Fig. 4a) and microscopic analysis (Fig. 4b). In the visual demonstration, red food dye mixed with water is clearly shown to rise through a clear pipette tip in Fig. 4a (See Online Resource 3). It was also shown that the fluid flow could be stopped and started by switching the transducer on and off as shown in Online Resource 4. This demonstrates the on-demand characteristic of the micropump. A smooth and bubble free pumping characteristic is also shown in

Online Resource 5 in which an initially empty microchannel is filled with a continuous fluid medium through pumping action. The pumping flow rate at different voltages was calculated through particle tracing analysis. The tracking of microparticles inside the channel is shown in Fig. 4b. Starting with the smallest applied voltage of 2 volts that could generate a net flow, the pumping flow rates of water were characterized as shown in Fig. 5. With the current device design and geometry, a pumping rate over 515 $\mu\text{l}/\text{min}$ was achieved at 12 volts applied voltage. At the highest voltage, the system drew only 0.15 Amps of current resulting in approximately a power value of 1.8 watts. At lower voltages, the flow rate could be decreased as desired. It is also important to note that some bio applications with delicate cell samples may require flow rates lower than the ones shown in Fig. 5. In the current device, off-the-shelf components were used which had fixed hole dimensions and numbers in the arrays. With customization of the geometry of these hole arrays, it can be possible to decrease or increase the achievable flow rates. For example, with smaller diameter holes, a much lower flow rate can be obtained. Another approach would be adding flow restricting features to the 3D printed parts to limit the flow rates for achieving much lower flow rates.

Compared to the previously shown acoustically driven micropumps as shown in Table 1 (Tovar et al. 2011; Huang et al. 2014; Wu et al. 2019; Yen et al. 2019; Ozelik and Aslan 2021), this system can provide a much higher flow rate at a minimal input power. This is a very important advantage

Fig. 3 Microscope images of the nozzle and diffuser sides of the metal sheet (membrane). a and b) Diffuser side of the membrane featuring 50 μm holes. c and d) Nozzle side of the membrane with 6 μm diameter holes

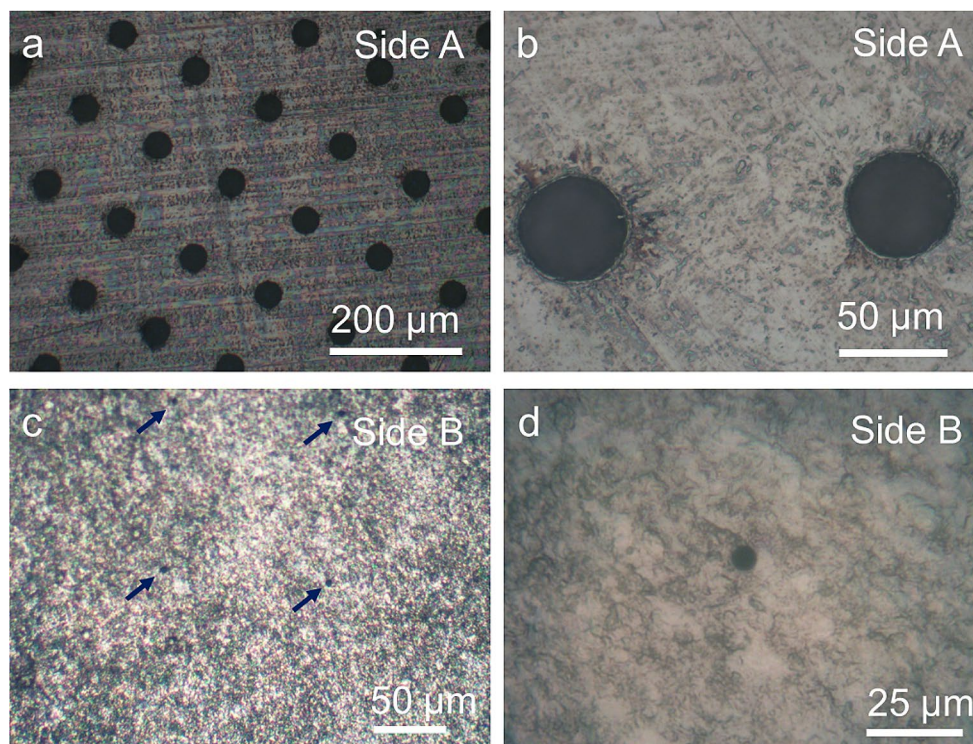


Fig. 4 Demonstration of fluid pumping. (a) Visual demonstration of the water colored with red food dye pumped through a clear pipette tip. (b) Image sequence of tracing of particles pumped inside a glass capillary

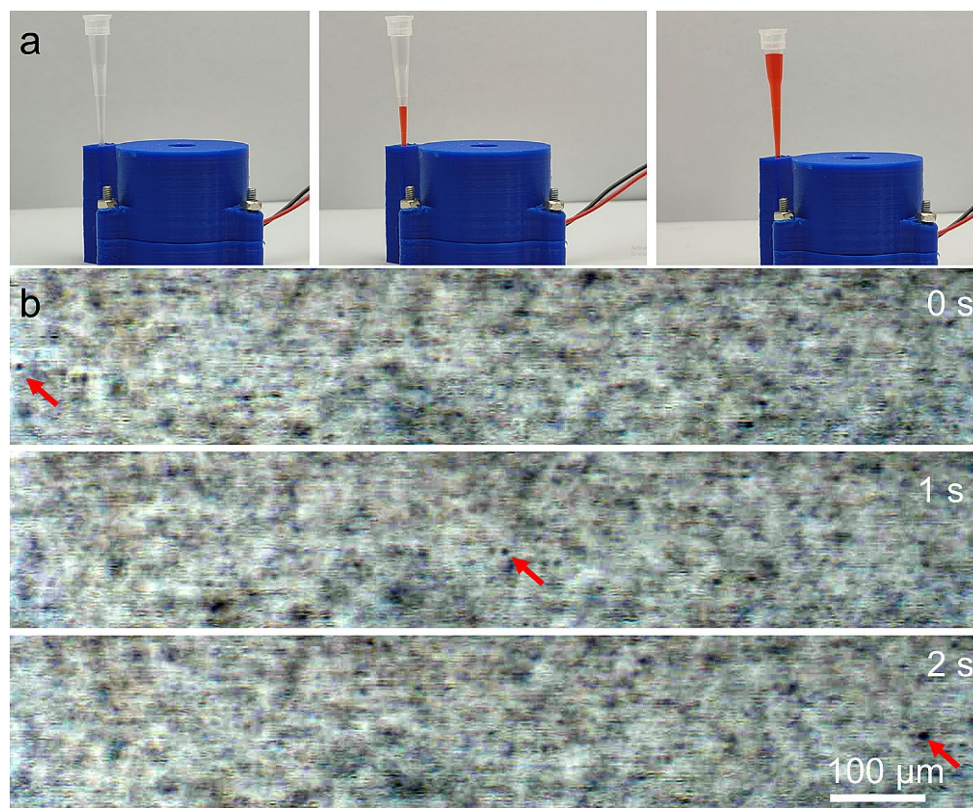


Fig. 5 Characterization of pumping flow rate as a function of applied voltages. Error bars represent the standard deviation of at least 5 measurements

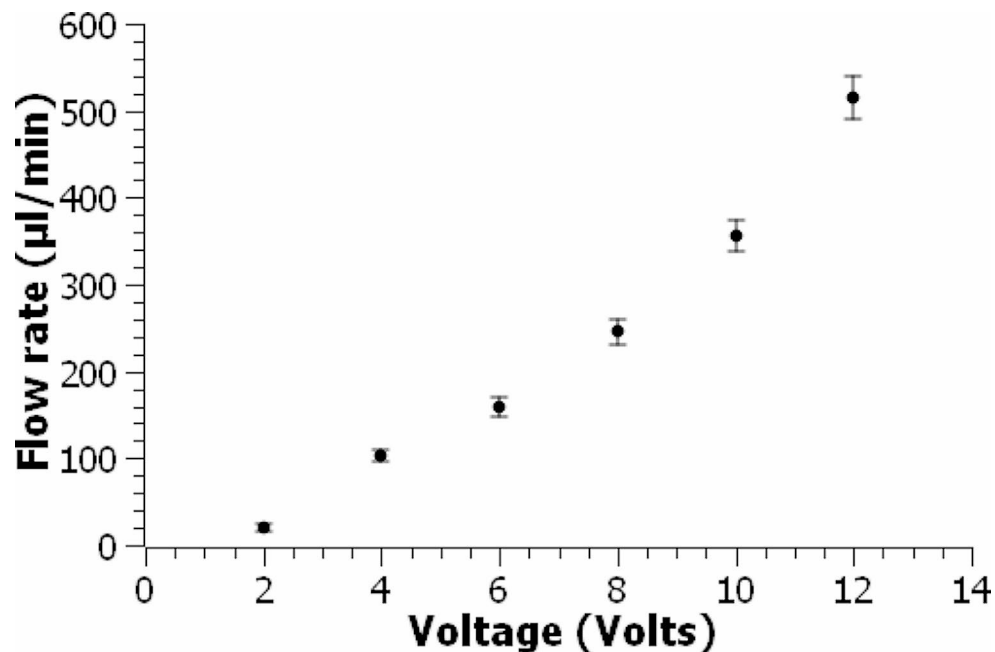


Table 1 Pumping performance comparison of some of the existing acoustofluidic micropumps

Working mechanism	Max flow rate	Required input	Reference
Valveless flow manipulation using a nozzle-shaped actuation chamber with acoustic resonator profile.	80 $\mu\text{l}/\text{min}$	60 volts	(Wang et al. 2010)
Acoustically driven, angled lateral air cavities	4.6 $\mu\text{l}/\text{min}$	25 volts	(Tovar et al. 2011)
Selective actuation of different sized microbubbles for bidirectional pumping	1.2 $\mu\text{l}/\text{min}$	7 volts	(Gao et al. 2020a)
Acoustofluidic stick-and-play micropump built on foil	0.42 $\mu\text{l}/\text{min}$	4 volts	(Lin et al. 2019b)
Acoustically driven tilted sharp-edge structures	8 $\mu\text{l}/\text{min}$	50 volts	(Huang et al. 2014)

Table 2 Comparison of some of the existing 3D printed micropumps

Working mechanism	Max flow rate	Required input	Reference
3D printed Quake-style valve-based micropump	120 $\mu\text{l}/\text{min}$	5 volts	(Lee et al. 2018)
Electro-magnetically actuated diffuser/nozzle pump	2.2 $\mu\text{l}/\text{min}$	Not reported	(Thomas et al. 2016)
Acoustic streaming within glass capillaries attached to 3D printed adaptors	12 $\mu\text{l}/\text{min}$	40 volts	(Ozcelik and Aslan 2021)
3D printed valve-based micropump	40 $\mu\text{l}/\text{min}$	Pressure-driven	(Gong et al. 2016)

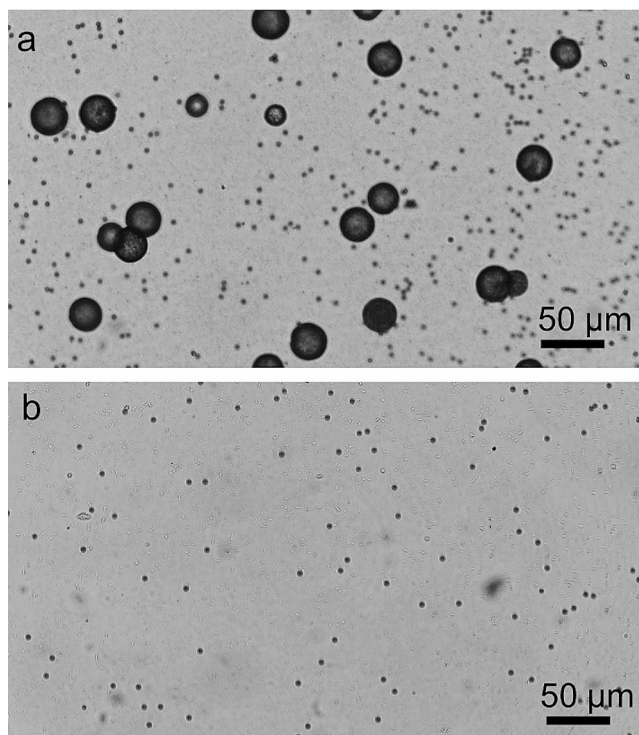


Fig. 6 Demonstration of particle filtration effect using the acoustic nozzle diffuser microfluidic pump. (a) A sample image of the fluid mixture containing 5 μm and larger polystyrene microparticles between 20 and 40 μm diameter. (b) The image of the sample fluid collected from the micropump

that shows the potential of the presented pump for a variety of lab-on-chip applications. In addition, this micropump is extremely simple, assembled with no microfabrication requirement, and can be replicated in any lab with a low-cost consumer-grade 3D printer. As compared to the majority of the 3D printed micropumps, the developed system also shows superiority in terms of performance (Table 2).

3.3 Filtration effect of the micropump

The presented micropump implements conic-shaped micro holes on a metal sheet that drive fluid from one side to the other in the diffuser direction through 113 kHz oscillations. Thanks to the very small size of the nozzle outlet, only particles larger than the diameter of the smaller hole can pass through the device. In this case, the hole is about 6 μm in diameter, and it should not let larger particles pass through the micropump. We tested this by using a mixture of 5 μm

microparticles and microparticles between 20 and 40 μm in diameter that were available in our lab. It was observed that only 5 μm particles passed through the device and larger particles were filtered out as shown in Fig. 6. A full reservoir of water mixture which was more than 6 ml was pumped through the device without any significant change in flow rate which showed that the larger particles did not cause any device clogging. It is possible that the high frequency (113 kHz) vibration of the metal membrane prevented clogging of the holes of the device and enabled continuous flow pumping. This feature of the micropump can be highly useful for biomedical applications where larger debris and unwanted impurities can be prevented from entering the microfluidic device. It can potentially even be used for separating larger cells and pumping only smaller ones into a microfluidic device for bioanalysis. We directly implemented commercially available standard transducers with metal sheet cover but it is also possible to optimize the dimensions of the conic-shaped holes to enable different filtration needs in addition to microfluidic flow control.

4 Conclusions

The field of miniaturized on-chip sample preparation and analysis systems has long needed compact and affordable fluid handling solutions. Despite the development of multiple microfluidic pumps, the search for a simple and cost-effective option has proven to be a difficult task. However, our study presents a simple micropump that meets these criteria and more. With the ability to achieve a wide range of flow rates, with a maximum of 515 $\mu\text{l}/\text{min}$, using a modest power input of 12 volts and 1.8 watts, this micropump is versatile. The underlying operating principle of this micropump revolves around an acoustic nozzle-diffuser mechanism. Notably, the entire fabrication and assembly process can be accomplished without the need for a cleanroom environment, enhancing accessibility for researchers and practitioners. Furthermore, the micropump demonstrates an additional capability for selective filtration of microparticles. This is achieved through the conic-shaped micro-holes that inhibit the passage of particles larger than the nozzle opening diameter, set at 6 μm in this study.

It is noteworthy that off-the-shelf components were exclusively utilized for the transducer and the controller in

this research. However, the micropump's potential for customization is highlighted, encouraging further exploration into the impact of varying the size and shape of the nozzle-diffuser microstructure on pumping performance. This can be achieved by tailoring the metal sheet cover on the transducer, providing a pathway for optimization based on specific application requirements. For wider accessibility, we encourage other researchers to replicate and assemble the micropump using the provided STL files, in conjunction with a readily available, low-cost control board and transducer kit. The simplicity in design, combined with its cost-effectiveness and versatility, positions this micropump as a valuable tool for on-chip applications. As we share this innovation with the community, we envision its potential to significantly contribute to advancements in various fields owing to its user-friendly attributes and practical utility.

Supplementary Information The online version contains supplementary material available at <https://doi.org/10.1007/s10404-024-02722-2>.

Acknowledgements We thank Fatih Akkoyun for the fruitful discussions regarding the device design.

Author contributions A.O. conceptualized the idea. A.O., S.G., E.Y., and I.E. contributed to the experimental work and data analysis. All authors contributed to the manuscript writing and editing.

Funding Open access funding provided by the Scientific and Technological Research Council of Türkiye (TÜBİTAK).

Data availability Data is provided within the manuscript or supplementary information files.

Code availability Code availability

Declarations

Competing interests The authors declare no competing interests.

Open Access This article is licensed under a Creative Commons Attribution 4.0 International License, which permits use, sharing, adaptation, distribution and reproduction in any medium or format, as long as you give appropriate credit to the original author(s) and the source, provide a link to the Creative Commons licence, and indicate if changes were made. The images or other third party material in this article are included in the article's Creative Commons licence, unless indicated otherwise in a credit line to the material. If material is not included in the article's Creative Commons licence and your intended use is not permitted by statutory regulation or exceeds the permitted use, you will need to obtain permission directly from the copyright holder. To view a copy of this licence, visit <http://creativecommons.org/licenses/by/4.0/>.

References

- Ahmadian MT, Mehrabian A (2006) Design optimization by numerical characterization of fluid flow through the valveless diffuser micropumps. *J Phys Conf Ser* 34:379–384. <https://doi.org/10.1088/1742-6596/34/1/062>
- Akkoyun F, Ozelik A (2022) A battery-powered fluid Manipulation System actuated by mechanical vibrations. *Actuators* 11:116. <https://doi.org/10.3390/act11050116>
- Akkoyun F, Gucluer S, Ozelik A (2021) Potential of the acoustic micromanipulation technologies for biomedical research. *Biomicrofluidics* 15. <https://doi.org/10.1063/5.0073596>
- Ao Z, Cai H, Wu Z et al (2021) Controllable fusion of human brain organoids using acoustofluidics. *Lab Chip* 21:688–699. <https://doi.org/10.1039/D0LC01141J>
- Ao Z, Cai H, Wu Z et al (2022) Human spinal organoid-on-a-Chip to Model Nociceptive Circuitry for Pain therapeutics Discovery. *Anal Chem* 94:1365–1372. <https://doi.org/10.1021/acs.analchem.1c04641>
- Bart SF, Tavrow LS, Mehregany M, Lang JH (1990) Microfabricated electrohydrodynamic pumps. *Sens Actuators Phys* 21:193–197. [https://doi.org/10.1016/0924-4247\(90\)85037-5](https://doi.org/10.1016/0924-4247(90)85037-5)
- Berthier E, Beebe DJ (2007) Flow rate analysis of a surface tension driven passive micropump. *Lab Chip* 7:1475. <https://doi.org/10.1039/b707637a>
- Binsley JL, Martin EL, Myers TO et al (2020) Microfluidic devices powered by integrated elasto-magnetic pumps. *Lab Chip* 20:4285–4295. <https://doi.org/10.1039/D0LC00935K>
- Bruus H (2012) Acoustofluidics 7: the acoustic radiation force on small particles. *Lab Chip* 12:1014. <https://doi.org/10.1039/c2lc21068a>
- Cai H, Ao Z, Wu Z et al (2021) Intelligent acoustofluidics enabled mini-bioreactors for human brain organoids. *Lab Chip* 21:2194–2205. <https://doi.org/10.1039/D1LC00145K>
- Chao S, Meldrum DR (2009) Spontaneous, oscillatory liquid transport in surface tension-confined microfluidics. *Lab Chip* 9:867. <https://doi.org/10.1039/b819887j>
- Chen Z, Noh S, Prisby RD, Lee JB (2020) An implanted magnetic microfluidic pump for in vivo bone remodeling applications. *Micromachines (Basel)* 11:1–10. <https://doi.org/10.3390/mi11030300>
- Cook SR, Musgrove HB, Throckmorton AL, Pompano RR (2022) Microscale impeller pump for recirculating flow in organ-on-chip and microreactors. *Lab Chip* 22:605–620. <https://doi.org/10.1039/D1LC01081F>
- Doinikov AA, Gerlt MS, Pavlic A, Dual J (2020) Acoustic streaming produced by sharp-edge structures in microfluidic devices. *Microfluid Nanofluidics* 24:32. <https://doi.org/10.1007/s10404-020-02335-5>
- Friend J, Yeo LY (2011) Microscale acoustofluidics: Microfluidics driven via acoustics and ultrasonics. *Rev Mod Phys* 83:647–704. <https://doi.org/10.1103/RevModPhys.83.647>
- Gandotra R, Kuo F-C, Lee MS, Lee G-B (2023) A paper-based aptamer-sandwich assay for detection of HNP 1 as a biomarker for periprosthetic joint infections on an integrated microfluidic platform. *Anal Chim Acta* 1281:341879. <https://doi.org/10.1016/j.aca.2023.341879>
- Gao Y, Wu M, Lin Y et al (2020a) Acoustic bubble-based bidirectional micropump. *Microfluid Nanofluidics* 24:29. <https://doi.org/10.1007/s10404-020-02334-6>
- Gao Y, Wu M, Lin Y, Xu J (2020b) Acoustic microfluidic separation techniques and bioapplications: a review. *Micromachines (Basel)* 11:921. <https://doi.org/10.3390/mi1100921>
- Gong H, Woolley AT, Nordin GP (2016) High density 3D printed microfluidic valves, pumps, and multiplexers. *Lab Chip* 16:2450–2458. <https://doi.org/10.1039/C6LC00565A>
- Gucluer S (2021) A battery powered on-chip peristaltic pump for Lab-On-A-Chip applications. *Eur Mech Sci* 5:201–205. <https://doi.org/10.26701/ems.876597>
- Guerra-Bravo E, Lee H-J, Baltazar A, Loh KJ (2021) Vibration analysis of a Piezoelectric Ultrasonic atomizer to Control Atomization Rate. *Appl Sci* 11:8350. <https://doi.org/10.3390/app11188350>

- Guo W, Hansson J, van der Wijngaart W (2018) Capillary pumping independent of the liquid surface energy and viscosity. *Microsyst Nanoeng* 4:2. <https://doi.org/10.1038/s41378-018-0002-9>
- Hanasoge S, Hesketh PJ, Alexeev A (2018) Microfluidic pumping using artificial magnetic cilia. *Microsyst Nanoeng* 4:11. <https://doi.org/10.1038/s41378-018-0010-9>
- Hossain MR, Dutta D, Islam N, Dutta P (2018) Review: electric field driven pumping in microfluidic device. *Electrophoresis* 39:702–731. <https://doi.org/10.1002/elps.201700375>
- Huang P-HH, Nama N, Mao Z et al (2014) A reliable and programmable acoustofluidic pump powered by oscillating sharp-edge structures. *Lab Chip* 14:4319–4323. <https://doi.org/10.1039/C4LC00806E>
- Iverson BD, Garimella SV (2008) Recent advances in microscale pumping technologies: a review and evaluation. *Microfluid Nanofluidics* 5:145–174. <https://doi.org/10.1007/s10404-008-0266-8>
- Jeong GS, Oh J, Kim SB et al (2014) Siphon-driven microfluidic passive pump with a yarn flow resistance controller. *Lab Chip* 14:4213–4219. <https://doi.org/10.1039/C4LC00510D>
- Karlsen JT, Augustsson P, Bruus H (2016) Acoustic force density acting on inhomogeneous fluids in Acoustic Fields. *Phys Rev Lett* 117:114504. <https://doi.org/10.1103/PhysRevLett.117.114504>
- Leach J, Mushfique H, di Leonardo R et al (2006) An optically driven pump for microfluidics. *Lab Chip* 6:735. <https://doi.org/10.1039/b601886f>
- Lee Y-S, Bhattacharjee N, Folch A (2018) 3D-printed quake-style microvalves and micropumps. *Lab Chip* 18:1207–1214. <https://doi.org/10.1039/C8LC00001H>
- Li S, Liu J, Jiang D (2013) Dynamic characterization of a Valveless Micropump considering Entrapped Gas bubbles. *J Heat Transf* 135. <https://doi.org/10.1115/1.4024461>
- Li L, Wang X, Pu Q, Liu S (2019) Advancement of electroosmotic pump in microflow analysis: a review. *Anal Chim Acta* 1060:1–16. <https://doi.org/10.1016/j.aca.2019.02.004>
- Li P-R, Kiran S, Wang C-H et al (2023a) A self-driven, microfluidic, integrated-circuit biosensing chip for detecting four cardiovascular disease biomarkers. *Biosens Bioelectron* 115931. <https://doi.org/10.1016/j.bios.2023.115931>
- Li W, Zhuge W, Jiang Y et al (2023b) A compact modularized power-supply system for stable flow generation in microfluidic devices. *Microfluid Nanofluidics* 27:80. <https://doi.org/10.1007/s10404-023-02693-w>
- Lin Y, Gao C, Gao Y et al (2019a) Acoustofluidic micromixer on lab-on-a-foil devices. *Sens Actuators B Chem* 287:312–319. <https://doi.org/10.1016/j.snb.2019.02.050>
- Lin Y, Gao Y, Wu M et al (2019b) Acoustofluidic stick-and-play micropump built on foil for single-cell trapping. *Lab Chip* 19:3045–3053. <https://doi.org/10.1039/c9lc00484j>
- Lu T-H, Chiang N-J, Tsai Y-C et al (2022) An integrated microfluidic system for cholangiocarcinoma diagnosis from bile by using specific affinity probes. *Sens Actuators B Chem* 373:132724. <https://doi.org/10.1016/j.snb.2022.132724>
- Nama N, Huang P-HH, Huang TJ, Costanzo F (2014) Investigation of acoustic streaming patterns around oscillating sharp edges. *Lab Chip* 14:2824–2836. <https://doi.org/10.1039/c4lc00191e>
- Neild A (2016) Motion controlled by sound. *Nature* 537:493–494. <https://doi.org/10.1038/537493a>
- Nisar A, Afzulpurkar N, Tuantranont A, Mahaisavariya B (2008) Three dimensional transient multifield analysis of a Piezoelectric Micropump for Drug Delivery System for treatment of hemodynamic dysfunctions. *Cardiovasc Eng* 8:203–218. <https://doi.org/10.1007/s10558-008-9060-1>
- Ozcelik A, Aslan Z (2021) A practical microfluidic pump enabled by acoustofluidics and 3D printing. *Microfluid Nanofluidics* 25:5. <https://doi.org/10.1007/s10404-020-02411-w>
- Ozcelik A, Aslan Z (2022) A simple acoustofluidic device for on-chip fabrication of PLGA nanoparticles. *Biomicrofluidics* 16. <https://doi.org/10.1063/5.0081769>
- Resto PJ, Berthier E, Beebe DJ, Williams JC (2012) An inertia enhanced passive pumping mechanism for fluid flow in microfluidic devices. *Lab Chip* 12:2221–2228. <https://doi.org/10.1039/c2lc20858j>
- Singhal V, Garimella SV, Murthy JY (2004) Low Reynolds number flow through nozzle-diffuser elements in valveless micropumps. *Sens Actuators Phys* 113:226–235. <https://doi.org/10.1016/j.sna.2004.03.002>
- Thomas DJ, Tehrani Z, Redfearn B (2016) 3-D printed composite microfluidic pump for wearable biomedical applications. *Addit Manuf* 9:30–38. <https://doi.org/10.1016/j.addma.2015.12.004>
- Tovar AR, Patel MV, Lee AP (2011) Lateral air cavities for microfluidic pumping with the use of acoustic energy. *Microfluid Nanofluidics* 10:1269–1278. <https://doi.org/10.1007/s10404-010-0758-1>
- Vafaei RH, Ghavifekr HB, Van Lintel H et al (2016) Bi-directional ACET micropump for on-chip biological applications. *Electrophoresis* 37:719–726. <https://doi.org/10.1002/elps.201500404>
- Wang SS, Huang XY, Yang C (2010) Valveless micropump with acoustically featured pumping chamber. *Microfluid Nanofluidics* 8:549–555. <https://doi.org/10.1007/s10404-009-0533-3>
- Wang T, Ni Q, Crane N, Guldiken R (2017) Surface acoustic wave based pumping in a microchannel. *Microsyst Technol* 23:1335–1342. <https://doi.org/10.1007/s00542-016-2880-9>
- Wu Z, Cai H, Ao Z et al (2019) A Digital Acoustofluidic Pump powered by localized fluid-substrate interactions. *Anal Chem* 91:7097–7103. <https://doi.org/10.1021/acs.analchem.9b00069>
- Wu M, Gao Y, Luan Q et al (2023a) Three-dimensional lab-on-a-foil device for dielectrophoretic separation of cancer cells. <https://doi.org/10.1002/elps.202200287>. *Electrophoresis*
- Wu T-H, Tsai Y-C, Kuo F-C et al (2023b) A microfluidic platform for detection and quantification of two biomarkers for rheumatoid arthritis. *Sens Actuators B Chem* 383:133587. <https://doi.org/10.1016/j.snb.2023.133587>
- Wu Z, Cai H, Tian C et al (2023c) Exploiting sound for emerging applications of extracellular vesicles. *Nano Res.* <https://doi.org/10.1007/s12274-023-5840-6>
- Xu L, Wang A, Li X, Oh KW (2020) Passive micropumping in microfluidics for point-of-care testing. *Biomicrofluidics* 14. <https://doi.org/10.1063/5.0002169>
- Yen P-W, Lin S-C, Huang Y-C et al (2019) A low-power CMOS microfluidic pump based on travelling-Wave Electroosmosis for Diluted serum pumping. *Sci Rep* 9:14794. <https://doi.org/10.1038/s41598-019-51464-7>
- Zhang C, Xing D, Li Y (2007) Micropumps, microvalves, and micromixers within PCR microfluidic chips: advances and trends. *Biotechnol Adv* 25:483–514. <https://doi.org/10.1016/j.biotechadv.2007.05.003>
- Zhang J, Yan Q, Huang J, Wu C (2018) Experimental Verification of the Pumping Effect caused by the Micro-tapered Hole in a Piezoelectric atomizer. *Sensors* 18:2311. <https://doi.org/10.3390/s18072311>
- Zhao B, Cui X, Ren W et al (2017) A controllable and Integrated pump-enabled Microfluidic Chip and its application in droplets Generating. *Sci Rep* 7:11319. <https://doi.org/10.1038/s41598-017-10785-1>
- Zhao F, Chen X, Zhang J et al (2021) A wearable, nozzle/diffuser microfluidic pump based on highperformance ferroelectric nanocomposites. *Sens Actuators B Chem* 347:130611. <https://doi.org/10.1016/j.snb.2021.130611>